Apoptosis (2019) 24:703–717
https://doi.org/10.1007/s10495-019-01551-x

ATP induces caspase-3/gasdermin E-mediated pyroptosis in NLRP3 pathway-blocked murine macrophages

Chen-Ying Zeng[1] · Chen-Guang Li[1] · Jun-Xiang Shu[1] · Li-Hui Xu[2] · Dong-Yun Ouyang[1] · Feng-Yi Mai[1] · Qiong-Zhen Zeng[1] · Cheng-Cheng Zhang[1] · Rui-Man Li[3] · Xian-Hui He[1]

Published online: 7 June 2019

Abstract

ATP acts as a canonical activator to induce NLRP3 (NOD-like receptor family, pyrin domain containing 3) inflammasome activation in macrophages, leading to caspase-1/gasdermin D (GSDMD)-mediated pyroptosis. It remains unclear whether ATP can induce pyroptosis in macrophages when the NLRP3 pathway is blocked by pathogenic infection. In this study, we used cellular models to mimic such blockade of NLRP3 activation: bone marrow-derived macrophages (BMDMs) treated with NLRP3-specific inhibitor MCC950 and RAW264.7 cells deficient in ASC (apoptosis-associated speck-like protein containing a caspase recruitment domain) expression. The results showed that ATP treatment induced lytic cell death morphologically resembling canonical pyroptosis in both MCC950-treated BMDMs and RAW264.7 cells, but did not cause the activation of caspase-1 (by detecting caspase-1p10 and mature interleukin-1β) and cleavage of GSDMD. Instead, both apoptotic initiator (caspase-8 and -9) and executioner (caspase-3 and -7) caspases were evidently activated and gasdermin E (GSDME) was cleaved to generate its N-terminal fragment (GSDME-NT) which executes pyroptosis. The GSDME-NT production and lytic cell death induced by ATP were diminished by caspase-3 inhibitor. In BMDMs without MCC950 treatment, ATP induced the formation of ASC specks which were co-localized with caspase-8; with MCC950 treatment, however, ATP did not induced the formation of ASC specks. In RAW264.7 cells, knockdown of GSDME by small interfering RNA attenuated ATP-induced lytic cell death and HMGB1 release into culture supernatants. Collectively, our results indicate that ATP induces pyroptosis in macrophages through the caspase-3/GSDME axis when the canonical NLRP3 pathway is blocked, suggestive of an alternative mechanism for combating against pathogen evasion.

Keywords Pyroptosis · Caspase-3 · Gasdermin E · ATP · Macrophages

Introduction

Innate immune cells sense pathogenic infection or tissue injury by recognizing pathogen-associated molecular patterns (PAMPs) and damage-associated molecular patterns (DAMPs), respectively, through a wide range of pattern recognition receptors (PRRs) [1–4]. Among them, macrophages are tissue-resident sentinels that survey their environments for potential infection or cellular injury via PRRs including membrane bound Toll-like receptors (TLRs) or cytosolic NOD-like receptors (NLRs) [5]. Recognition of PAMPs by TLRs induces signaling transduction of the NF-κB pathway culminating in expression of pro-inflammatory cytokines, while activation of cytosolic PRRs such as NLRP3 (NOD-like receptor family, pyrin domain containing 3) leads to the formation of multiple protein complex named inflammasome [3].

Electronic supplementary material The online version of this article (https://doi.org/10.1007/s10495-019-01551-x) contains supplementary material, which is available to authorized users.

Chen-Ying Zeng, Chen-Guang Li and Jun-Xiang Shu are contributed equally to this work.

✉ Rui-Man Li
hqyylrm@126.com

✉ Xian-Hui He
thexh@jnu.edu.cn

[1] Department of Immunobiology, College of Life Science and Technology, Jinan University, Guangzhou, China

[2] Department of Cell Biology, College of Life Science and Technology, Jinan University, Guangzhou, China

[3] Department of Gynecology and Obstetrics, The First Affiliated Hospital of Jinan University, Guangzhou, China

The formation of NLRP3 inflammasome can be triggered by a variety of DAMPs, PAMPs, or environmental irritants [6, 7]. Extracellular ATP is a DAMP that activates NLRP3 inflammasome by triggering K^+ efflux via binding to purinergic P2X7 receptor (P2X7R) [8]. ATP-P2X7R-induced K^+ efflux and activation of NLRP3 inflammasome has recently been reported to be mediated by TWIK2 (two-pore domain weak inwardly rectifying K^+ channel 2) [9]. The triggering of NLRP3 leads to the recruitment of adaptor ASC (apoptosis-associated speck-like protein containing a caspase recruitment domain) and pro-caspase-1 to form a large multi-protein NLRP3 inflammasome resulting in the autocatalytic activation of caspase-1 [3, 6, 7]. Activated caspase-1 in turn cleaves gasdermin D (GSDMD, a member of gasdermin family) into C-terminal and N-terminal (GSDMD-NT) fragments [10, 11]. GSDMD-NT binds to and forms pores on the plasma membrane, thereby causing pyroptosis—a rapid proinflammatory programmed cell death typified by cellular swelling, membrane disruption, and release of proinflammatory cytoplasmic contents including HMGB1 [12–20]. Pyroptosis is therefore regarded as a critical host defense mechanism against intracellular pathogenic bacteria by releasing them into the extracellular environment where they can be killed by neutrophils [21–23].

Apart from GSDMD, gasdermin E (GSDME)/DFNA5 (another member of the gasdermin family) has been shown to have a critical role in mediating pyroptotic/necrotic cell death [24, 25]. Upon apoptotic stimulation, cleavage of GSDME by activated caspase-3 leads to the production of GSDME-NT (~37 kDa), which also forms pores on the plasma membrane, and thereby transforms apoptosis into pyroptosis/necrosis. This caspase-3-mediated cleavage of GSDME has an important role in chemotherapy-induced tissue damage and cytotoxicity on the intestines because the intestinal epithelial cells express high levels of GSDME protein [24].

Inflammasome-mediated pyroptosis and cytokine release are critical defense against pathogenic microbes; successful pathogens have therefore evolved strategies to evade such mechanisms [26, 27]. For example, the *Yersinia* type II secretion effector YopM directly binds caspase-1 and sequesters it from inflammasome formation, thus blocking pyroptosis and IL-1β processing [28]. Virus-encoded proteins can also target inflammasome activation: myxoma virus and rabbit fibroma virus express PYD-containing proteins that bind to ASC thereby inhibiting caspase-1 activation and IL-1β secretion [29, 30]. Under such circumstances, the switch between different forms of cell death may have important physiological roles as an alternative mechanism in defending the host against evasion of pathogens. But it is still incompletely understood whether suppression of NLRP3/caspase-1-mediated conventional pyroptosis could switch to a different form of cell death.

In this study, we aimed to explore the cell death form in murine macrophages when the NLRP3 pathway was blocked. We found that pyroptosis was observed in mouse bone marrow-derived macrophages (BMDMs) with the NLRP3 inflammasome activation being inhibited by NLRP3-specific inhibitor MCC950 [31], upon ATP stimulation. Similar pyroptosis was observed in RAW 264.7 cell line that has deficiency in the NLRP3 pathway [14], in an alternative way depending on the caspase-3/GSDME axis. Our study highlights that ATP, acting as a DAMP during tissue injury or infections, may induce an alternative form of pyroptosis in macrophages when the NLRP3 inflammasome pathway has been blocked, suggestive of an alternative mechanism against pathogen evasion.

Materials and methods

Reagents and antibodies

Adenosine triphosphate (ATP) (A6419), lipopolysaccharide (LPS) (*Escherichia coli* O111:B4) (L4391), phorbol 12-myristate 13-acetate (PMA) (P8139), Tween-80 (P8074), and propidium iodide (P4170) were obtained from Sigma-Aldrich (St. Louis, MO, USA). ATP was freshly prepared by dissolving in phosphate-buffered saline (PBS). Nigericin (tlrl-nig) was obtained from InvivoGen (San Diego, CA, USA). Ac-DEVD-CHO (#HY-P1001) was bought from MedChem Express (Princeton, NJ, USA). MCC950 (#S7809) was from Selleck (Houston, TX, USA). Dulbecco's Modified Eagle's Medium (DMEM) with high glucose, RPMI 1640, β-mercaptoethanol, fetal bovine serum (FBS), Opti-MEM, streptomycin and penicillin were obtained from ThermoFisher/Gibco (Carlsbad, CA, USA). CytoTox 96 Non-Radioactive Cytotoxicity Assay kit was obtained from Promega (Madison, WI, USA). The antibody against NLRP3 (Cryo-2) (AG-20B-0014) was purchased from Adipogen AG (Liestal, Switzerland). Specific antibodies against HMGB1 (#3935), ASC (#67824), IL-1β (#12242), cleaved caspase-9 (#9509), cleaved caspase-7 (#8438), cleaved caspase-8 (#8592), PARP (#9532), cleaved caspase-3 (#9664), caspase-3 (#9665), ASC AlexaFluor488-conjugated (#17507), horse-radish peroxidase (HRP)-conjugated horse anti-mouse IgG (#7076), and HRP-conjugated goat-anti-rabbit IgG (#7074) were purchased from Cell Signaling Technology (Danvers, MA, USA). CF568-conjugated goat-anti-rabbit IgG (#20103) was purchased from Biotium (Hayward, CA, United States). The antibody against actin (sc-1616-R) was bought from Santa Cruz (Dallas, TX, USA). Rabbit monoclonal antibodies against pro-cspase1+p10+p12 (ab179515), caspase-8 (ab108333), GSDMD (ab209845), and DFNA5/GSDME (ab215191) were obtained from Abcam (Cambridge, UK).

Cell line and cell culture

RAW 264.7 and THP-1 cells were obtained from the Cell Bank of the Chinese Academy of Sciences (Shanghai, China). RAW 264.7 cells were maintained in DMEM supplemented with 10% FBS, 100 U/ml penicillin, 100 µg/ml streptomycin, and 2 mM L-glutamine (DMEM complete medium) while THP-1 cells were cultured in RPMI 1640 plus 10% FBS, 100 U/ml penicillin, 100 µg/ml streptomycin, 2 mM L-glutamine and 50 µM β-mercaptoethanol. Cells were incubated at 37 °C in a humidified incubator of 5% CO_2, and sub-cultured every 2–3 days. For induction of macrophages, THP-1 cells were planted in 96-well plates at 4×10^4 cells/well in 0.1 ml medium or in 24-well plates at 1.5×10^5 cells/well in 0.5 ml medium and treated with PMA (100 nM) for 24 h.

Bone marrow-derived macrophage culture

Bone marrow was derived from hind femora and tibias of C57BL/6 mice (6–8 weeks of age) obtained from the Experimental Animal Center of Southern Medical University (Guangzhou, China). Animal experiments were performed according to the guidelines for the care and use of animals approved by the Committee on the Ethics of Animal Experiments of Jinan University. BMDMs were differentiated as described previously [32]. In brief, bone marrow cells were differentiated in DMEM supplemented with 10% FBS, 100 U/ml penicillin, 100 µg/ml streptomycin and 20% M-CSF-conditioned medium from L-929 fibroblasts for 6 days. After 6 days, BMDMs were collected by using a cell scraper and then cultured in fresh DMEM complete medium overnight in 24-well plates at 1.5×10^5 cells/well in 0.5 ml or in 6-well plates at 1.5×10^6 cells/well in 2 ml.

Cell death assay

Cell death was measured by PI incorporation, which shows loss of plasma membrane integrity. The assay was performed essentially as described previously [33, 34]. In brief, cells were seeded in 24-well plates, stimulated with or without 500 ng/ml LPS for 4 h. Subsequently, the cells were treated with various concentrations of ATP for indicated time periods in Opti-MEM. PI (2 µg/ml) was added to cell culture media at room temperature for 10 min, then cells were observed immediately by live imaging using a Zeiss Axio Observer D1 microscope equipped with a Zeiss LD Plan-Neofluar 20×/0.4 Korr M27 objective lens. Fluorescence images were captured with a Zeiss AxioCam MR R3 cooled CCD camera controlled with ZEN software (Carl Zeiss MicroImaging GmbH, Göttingen, Germany). In some experiments, cell death was also measured by using LDH release assay (CytoTox 96 Non-Radioactive Cytotoxicity Assay), according to the manufacturer's instructions.

Measurement of soluble IL-1β

IL-1β in culture supernatants was measured by cytometric bead array (CBA) mouse IL-1β Flex Set (#560232) with the indicated buffer (#558266) (BD Biosciences, San Jose, CA, USA) according to the protocol provided by the supplier. Data were analyzed on a Attune NxT acoustic focusing cytometer (ThermoFisher Scientific, Carlsbad, CA, USA).

Immunofluorescence microscopy

Immunofluorescence microscopy was performed as previously reported [34]. In brief, BMDMs were planted in glass-bottom dishes at 1.2×10^6 cells/well in 1.5 ml and incubated at 37 °C overnight. After appropriate treatment, cells were fixed by 4% paraformaldehyde and permeabilized with methanol. Cells were blocked by blocking buffer and then incubated with anti-caspase-8 antibody followed by incubation with CF568-conjugated goat-anti-rabbit IgG and subsequently stained with AlexaFluor488-conjugated rabbit-anti-mouse ASC antibody. Nuclei were revealed by Hoechst 33342 staining (5 µg/ml in PBS). Fluorescent images of cells were captured under a Zeiss Axio Observer D1 microscope with a Zeiss LD Plan-Neofluar 100×/0.6 Korr M27 objective lens (Carl Zeiss MicroImaging GmbH, Göttingen, Germany).

Small interfering RNA (siRNA)

The siRNA (5′-GCTGCAAACTCCATGTTAT-3′, 5′-GTACGCGCACAAGCTAGAA-3′, and 5′-GTACTTAAATCGTGAAACA-3′ duplexes that target mouse GSMDE/DFNA5 caspase-3, and NLRP3, respectively) and negative control (NC) siRNA were designed and synthesized by RiboBio (Guangzhou, China). Transfection was performed using Lipofectamine RNAiMAX (ThermoFisher/Invitrogen) according to the manufacturer's instructions. In brief, before transfection, RAW 264.7 cells were plated in 6-well plates or 24-well plates at 30–50% confluency overnight, and in the next day, cells were transfected with GSDME siRNA (20 nM) or NC siRNA (20 nM). The cells were cultured in DMEM medium containing 10% FBS for 48 h, followed by stimulation with ATP (2 mM). Cell death was assayed by PI staining and fluorescent images were captured by fluorescence microscopy, merged with bright-field images. GSDME and HMGB1 expression levels were determined by using western blotting. For knockdown of *caspase-3* in RAW 264.7 cells, the siRNA concentrations were 50 nM for 48 h and the cells were ready for experiments. For

knockdown of *NLRP3*, RAW 264.7 cells were primed with LPS for 4 h and then siRNA (10 nM) was transfected into the cells for 48 h.

Precipitation of soluble proteins

Proteins in culture supernatants (equal volume for each sample) were precipitated overnight with 7.2% trichloroacetic acid plus 0.15% sodium deoxycholate as previously described [35, 36]. The precipitates were lysed in equal volume of 1× sodium dodecyl sulfate–polyacrylamide gel electrophoresis (SDS-PAGE) loading buffer and subjected to western blot analysis for HMGB1.

Western blot analysis

Western blotting was performed as previously described to detect proteins in cell lysates and supernatants, respectively [34]. In brief, equivalent proteins were separated by SDS-PAGE and then transferred onto a PVDF membrane (#03010040001; Roche Diagnostics GmbH, Mannheim, Germany). Then the membranes were blocked with blocking buffer [50 mM Tris-buffered saline (pH 7.4) containing 5% nonfat milk and 0.1% Tween-20] and incubated with primary antibodies at 4 °C overnight, followed by HRP-conjugated goat anti-rabbit IgG or goat anti-mouse IgG secondary antibody. The bands were revealed with an enhanced chemiluminescence kit [BeyoECL Plus (P0018); Beyotime, Shanghai, China] and recorded on X-ray films (Carestream, Xiamen, China). The densitometry of each band was quantified by FluorChem 8000 (Alpha Innotech; San Leandro, CA, USA).

Statistical analysis

Experiments were performed three times independently. Data were expressed as mean ± standard deviation (SD). Statistical analysis was performed using GraphPad Prism5.0 (GraphPad Software Inc., San Diego, CA, USA). Statistical evaluation was performed using Student's *t* test (two tailed) between two groups or one-way analysis of variance (ANOVA) followed by Tukey post hoc test for multiple comparison. *P*-values < 0.05 were considered statistically significant.

Results

Blockade of the NLRP3 pathway switches ATP-induced canonical pyroptosis to alternative pyroptosis in BMDMs

We sought to explore whether ATP could induce pyroptosis in primary macrophages with NLRP3 inflammasome activation being blocked. MCC950 is a specific inhibitor of NLRP3 inflammasome [31]. We used this inhibitor at a dose of 1 μM that can efficiently suppress NLRP3 inflammasome activation. Given that pyroptosis is a lytic form of cell death with loss of membrane integrity [22], we evaluated it (if there was) by analyzing the incorporation of PI into the cells. In the absence of MCC950, we found that ATP induced ~ 70% of lytic cell death, in LPS-primed BMDMs (Fig. 1a, b), concomitant with the production of caspase-1p10 and mature IL-1β as well as cleavage of GSDMD as revealed by Western blot analysis of combined cell lysates and precipitated proteins from culture supernatants (Fig. 1c). Prolonged incubation with ATP led to increased activation of caspase-1 (indicated by caspase-1p10) and production of mature IL-1β, but only weakly led to caspase-3 activation and GSDME-NT generation. Consistent with previous study [31], pre-treatment of MCC950 almost completely blocked ATP-induced lytic cell death at the time point of 1 h (Fig. 1a, b), accompanied by suppression of caspase-1p10, mature IL-1β, and GSDMD-NT production in comparison with vehicle treatment (Fig. 1c). However, when the incubation time was prolonged, ATP did induce lytic cell death with ballooning from the cells accompanied by the generation of GSDME-NT, but not GSDMD-NT and caspase-1p10 (Fig. 1a–c). The lytic cell death by PI staining was confirmed by LDH release assay (Supplementary Fig. 1a). Similar to Western blot analysis, bead-based assay (CBA) showed that ATP induced high levels of soluble IL-1β in the culture supernatants without MCC950 pre-treatment but only induced very low levels of IL-1β in those cells pre-treated with MCC950 (Supplementary Fig. 1b), thus confirming the results of Western blotting (Fig. 1c). Apoptotic cells (judged morphologically by their shrinkage and membrane blebbing) were also observed (Fig. 1b). In line with this, apoptotic caspases (caspase-8/-9/-3) were activated and poly-ADP ribose polymerase (PARP) was also cleaved to produce the 89 kDa fragment (Fig. 1c), corroborating apoptosis in the cells. Moreover, in the absence of MCC950, ATP treatment induced formation of ASC specks which were co-localized with caspase-8, consistent with previous observation [37]; in the presence of MCC950, however, ATP did not induce the formation of any ASC specks (Fig. 2), indicating complete blockade of NLRP3 inflammasome assembly.

Apart from ATP, another NLRP3 inducer nigericin [8] was used to trigger cell death in mouse BMDMs with or without MCC950 treatment. Without MCC950 pre-treatment, nigericin induced rapid cell death accompanied by the activation of caspase-1 and cleavage of GSDMD and pro-IL-1β; in the presence of MCC950, however, nigericin induced a delayed cell death accompanied by the activation of caspase-8/-9/-7/-3 and the cleavage of GSDME and PARP, but not cleavage of caspase-1, pro-IL-1β and GSDMD (Supplementary Fig. 2a–c). Besides, we also

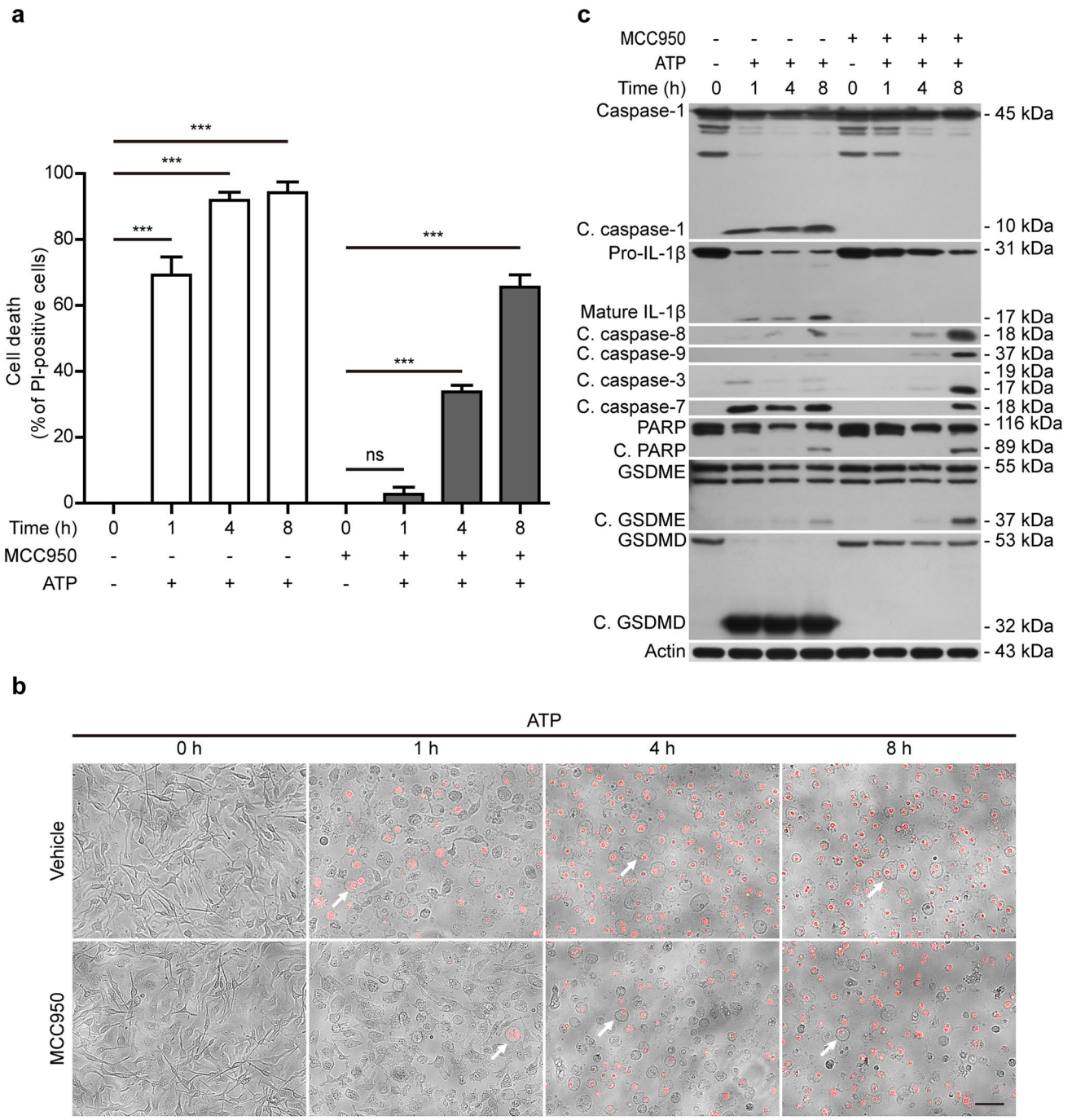

Fig. 1 Induction of a delayed lytic cell death by ATP in BMDMs pre-treated with MCC950. BMDMs were primed with LPS (500 ng/ml) for 4 h, pre-treated with or without MCC950 (1 μM) for 30 min and followed by stimulation with ATP (5 mM) for indicated time periods in the presence or absence of MCC950. **a** Histograms show the ratios of PI-positive cells quantified by counting five randomly chosen fields containing ~ 100 cells each. The percentage of lytic cell death is defined as the ratio of PI-positive cells relative to all cells. Data are shown as mean ± SD ($n = 5$). Statistical significance was analyzed by one-way ANOVA followed by Tukey post hoc test. ***$P < 0.001$. **b** Merged images showing PI fluorescence (red) combined with bright-field images. One set of representative images of three independent experiments are shown. Scale bar, 50 μm. The arrow in each image indicates a typical cell with ballooning morphology. **c** Combined precipitated proteins of culture supernatants and cell lysates were collected and Western blot analysis was used to assess the expression levels of indicated proteins in the combined samples. Actin was used as a loading control. *C* Cleaved, *ns* Not significant (Color figure online)

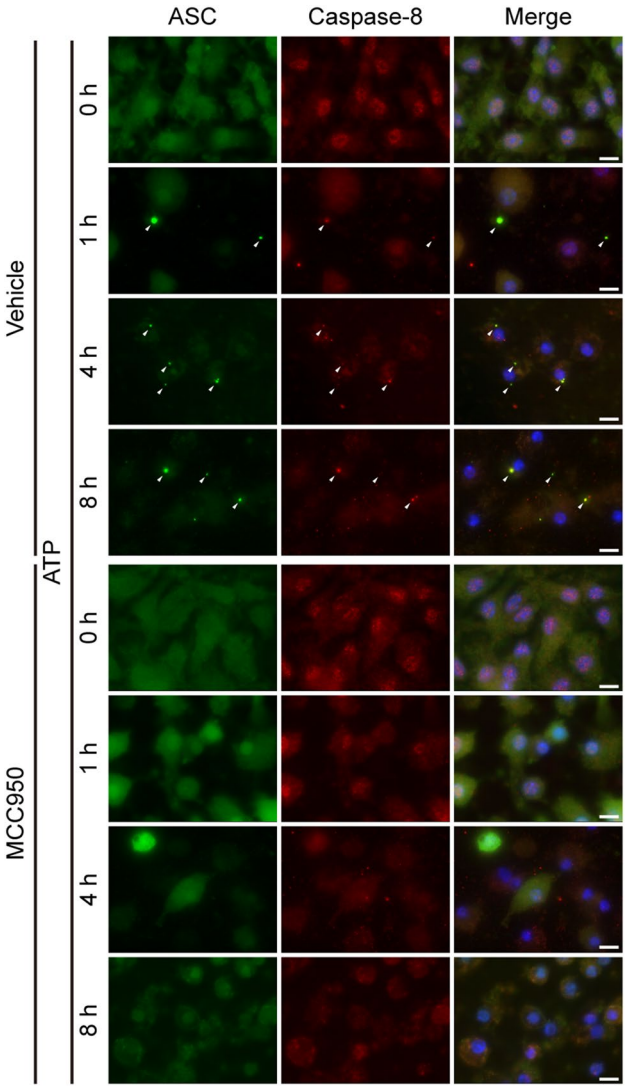

Fig. 2 Blockade of ATP-induced formation of ASC specks by MCC950 pre-treatment. BMDMs planted in glass-bottom dishes were primed with LPS (500 ng/ml) for 4 h, and pre-treated with or without MCC950 (1 μM) for 30 min, followed by stimulation with ATP (5 mM) for indicated time periods in the presence or absence of MCC950. After fixation and permeabilization, the cells were stained with anti-caspase-8 antibody and CF568-goat-anti-rabbit IgG, followed by AlexaFluor488 conjugated anti-ASC antibody. Nuclei were revealed by Hoechst 33342 staining. Fluorescence images were captured by fluorescence microscopy. Merge images with nuclei are also shown. Arrow heads indicate ASC specks which were co-localized with caspase-8. Scale bars, 10 μm

performed experiments in THP-1-derived macrophages, showing that nigericin could induce a delayed form of lytic cell death in the cells pre-treated with MCC950 (Supplementary Fig. 3a–c), suggesting similar phenomenon might occur in human macrophages. Together, these results suggested that blockade of NLRP3 inflammasome activation switched NLRP3-mediated rapid pyroptosis into apoptosis and delayed pyroptosis mediated by GSDME activation.

Fig. 3 Induction of lytic cell death by ATP in RAW 264.7 cells. Cells were primed with or without LPS (500 ng/ml) for 4 h, followed by stimulation with indicated concentrations of ATP. Cell death was assayed by PI staining for 10 min and images were captured by fluorescence microscopy. **a** Histograms showing ratios of PI-positive cells quantified by counting five randomly chosen fields (from 5 wells) each containing ~ 100 cells. The percentage of lytic cell death is defined as the ratio of PI-positive cells relative to all cells. Data are shown as mean ± SD ($n = 5$). Statistical significance was analyzed by one-way ANOVA followed by Tukey post hoc test. ***$P < 0.001$. **b** Merged images showing PI fluorescence (red) combined with bright-field (BF) images. RAW 264.7 cells were treated with ATP (2 mM) for 4 h. One set of representative images of three independent experiments is shown. Scale bar, 50 μm. The arrow in each magnified inset indicates a typical cell with a ballooning morphology. **c, d** Whole cell lysates were collected and Western blot analysis was used to assess the expression levels of indicated proteins in the cell lysates. Actin was used as a loading control. **e, f** Precipitated proteins of culture supernatants and whole cell lysates were collected, respectively, and Western blot analysis was used to assess the expression levels of indicated proteins. The positive control (PC) of caspase-1p10 and mature IL-1β was a sample of combined cell lysate and precipitated proteins of culture supernatant of LPS-primed BMDMs stimulated with ATP (5 mM) for 1 h. Actin was used as a loading control for cell lysates. *Indicates non-specific bands (Color figure online)

ATP induces alternative pyroptosis in RAW 264.7 cells defective in NLRP3 pathway

Consistent with the fact that RAW 264.7 macrophages are defective in the NLRP3 pathway due to deficiency in ASC expression [38], we next assessed whether ATP could induce alternative pyroptosis in this cell line. As expected, NLRP3-mediated pyroptosis was not induced in this cell line upon the stimulation of ATP within 1 h (Fig. 3a), which is the time commonly used for inducing pyroptosis in wild-type macrophages [8]. We thus prolonged the treatment time, and the results showed that ATP induced time- and dose-dependent lytic cell death in both unprimed and LPS-primed cells, while there was no cell death or only a minor fraction of dying cells in vehicle-treated cells (Fig. 3a). It is worth noting that more than 1 or 2 h were required for ATP to induce such lytic cell death (Fig. 3a). The dying cells had a swelling morphology resembling that of pyroptotic cells with ballooning from the cell membrane and loss of membrane integrity (Fig. 3b), suggesting that ATP had induced pyroptosis in RAW 264.7 cells.

We next investigated whether ATP had activated apoptotic or inflammatory caspases in RAW 264.7 cells. Western blot analysis showed that both apoptotic initiator caspases (caspase-8 and -9) and executioner caspases (caspase-3 and -7) were markedly activated in a time-dependent manner after prolonged ATP stimulation (Fig. 3c, d), and accordingly their substrate PARP was also cleaved to generate an 89 kDa fragment (Although PARP was markedly decreased after prolonged ATP treatment in LPS-primed cells (Fig. 3d), it is unclear why the 89 kDa fragment was invisible; one possibility is that it had been further degraded). As expected,

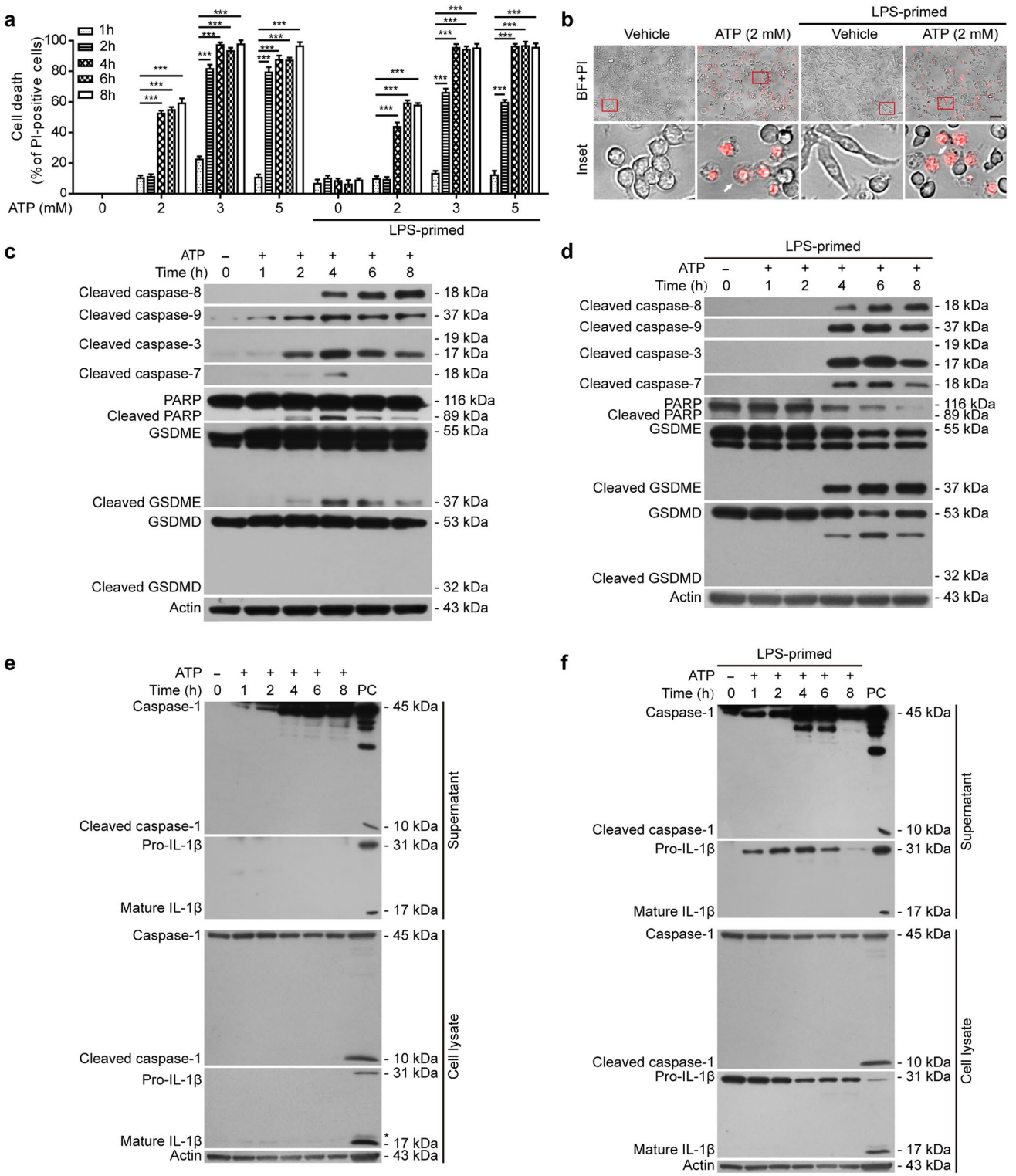

cleaved caspase-1p10 (a fragment of active caspase-1) was undetectable both in the cell lysates and in the culture supernatants even though pro-caspase-1 was detected in the supernatants (Fig. 3e, f). Consistent with the absence of caspase-1p10, GSDMD was not cleaved to generate GSDMD-NT (32 kDa) (Fig. 3c, d), and no mature IL-1β was detected in LPS-primed cell lysates and supernatants, although LPS-induced pro-IL-1β was detectable in the supernatants upon ATP stimulation (Fig. 3e, f). However, accompanying the robust activation of caspase-3 at later time points, GSDME

was cleaved to produce GSDME-NT (37 kDa) (Fig. 3c, d), which has recently been shown to mediate pyroptosis [24, 25]. These results suggested that prolonged treatment with ATP had induced caspase-3/GSDME- but not caspase-1/GSDMD-mediated pyroptosis in the cells lacking conventional NLRP3 activation.

Caspase-3 is involved in ATP-induced pyroptosis in macrophages with NLRP3 pathway being blocked

We next sought to verify the role of caspase-3 and GSDME in the alternative pyroptosis in BMDMs treated with ATP in the presence of MCC950 and in RAW 264.7 cells. To this end, we inhibited caspase-3 with its specific inhibitor Ac-DEVD-CHO (DEVD). The results showed that DEVD dose-dependently suppressed ATP-induced lytic cell death (Fig. 4a, b). The generation of GSDME-NT and PARP fragment in this process was also attenuated by DEVD (Fig. 4c). These results confirmed that active caspase-3 had been involved in the cleavage of GSDME, which had mediated such pyroptosis in macrophages upon ATP stimulation when the NLRP3 pathway was blocked.

Similarly, in RAW 264.7 cells, it was shown that ATP-induced lytic cell death was dramatically suppressed by caspase-3 inhibitor DEVD in a dose-dependent manner (Fig. 5a). Similar results were observed in ATP-induced cell death in LPS-primed cells (Fig. 5b). DEVD (100 μM) *per se* was unable to induce cell death or cell morphology change (data not shown). Then we knocked down caspase-3 expression in RAW 264.7 cells by siRNA. This significantly suppressed ATP-induced lytic cell death (Fig. 5c, d) and decreased the cleavage of GSDME and PARP (Supplementary Fig. 4), confirming the role of caspase-3 in this process. But, NLRP3 knockdown had minimal effect on the cell death (Fig. 5e, f), suggesting that NLRP3 knockdown was not necessary for blocking the inflammasome activation and

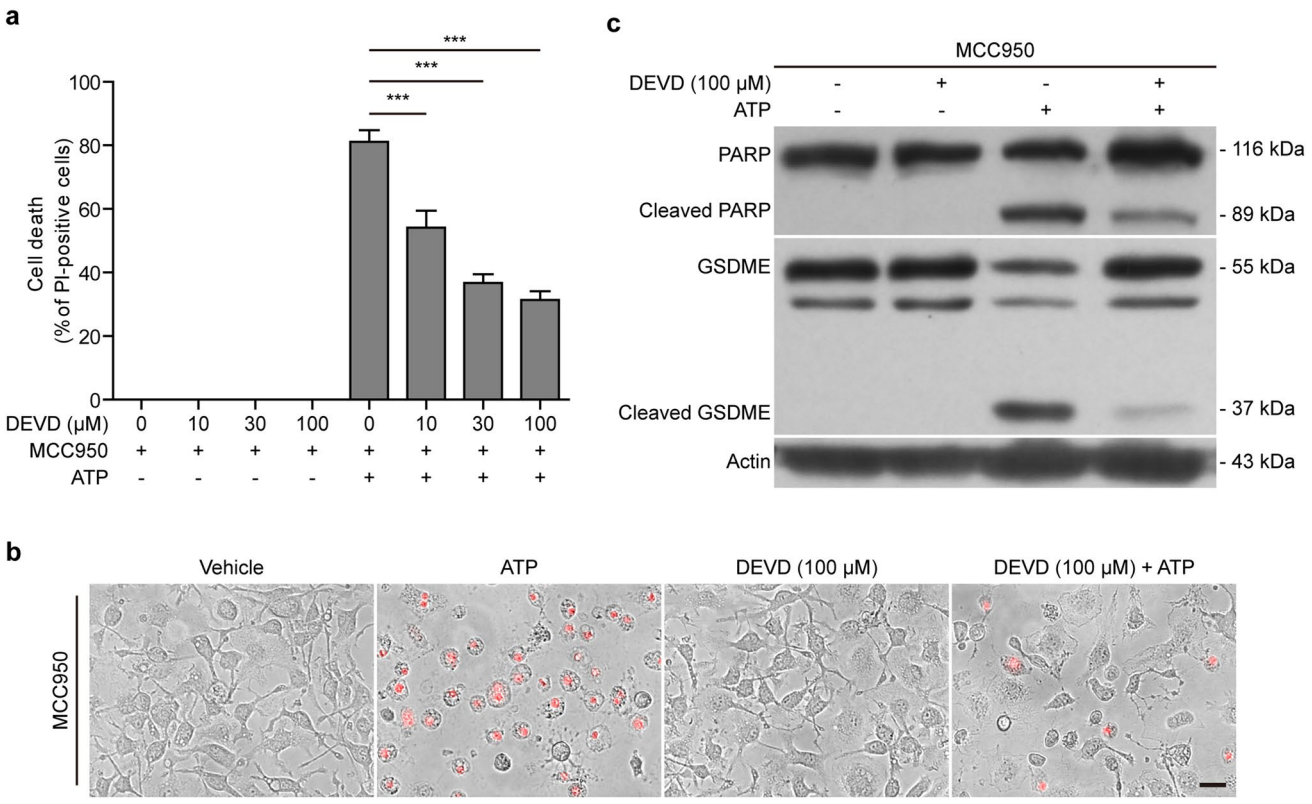

Fig. 4 Inhibition of caspase-3 attenuated ATP-induced lytic cell death concomitant with decreased cleavage of gasdermin E (GSDME) in BMDMs pre-treated with MCC950. BMDMs were first primed with LPS (500 ng/ml) for 4 h, pre-treated with or without MCC950 (1 μM) and caspase-3 inhibitor Ac-DEVD-CHO (DEVD) for 1 h and followed by stimulation with ATP (5 mM) in the presence or absence of MCC950. **a** Histograms show the ratios of PI-positive cells quantified by counting five randomly chosen fields containing ~ 100 cells each. The percentage of lytic cell death is defined as the ratio of PI-positive cells relative to all cells. Data are shown as mean ± SD ($n = 5$). Statistical significance was analyzed by one-way ANOVA followed by Tukey post hoc test. ***$P < 0.001$. **b** Merged images showing PI fluorescence (red) combined with bright-field images. One set of representative images of three independent experiments are shown. Scale bar, 20 μm. **c** The cell lysates were collected and Western blotting was performed to assess the expression levels of indicated proteins. Actin was used as a loading control (Color figure online)

GSDMD cleavage as ASC is deficient in RAW 264.7 cells. These results corroborated that the lytic cell death induced by ATP in RAW 264.7 cells was caspase-3/GSDME- but not GSDMD-mediated pyroptosis, in which active caspase-3 was a key executioner caspase leading to GSDME cleavage.

Knockdown of GSDME partly attenuates ATP-induced cell death

To further confirm the participation of GSDME in the lytic cell death induced by ATP, we genetically knocked down its expression in RAW 264.7 cells by siRNA. Western blotting showed that the expression of GSDME protein was reduced approximately 80% after knockdown (Fig. 6a). This significantly attenuated the lytic cell death upon ATP treatment in comparison to negative control (Fig. 6b, c). Morphologically, ATP-induced dying cells, either with or without GSDME knockdown, had similar ballooning and rounding phenotypes, resembling pyroptotic but not apoptotic cells (typified by cell shrinkage or membrane blebbing) (Fig. 6c). In addition, the release of HMGB1 (another DAMP that is associated with lytic cell death) in the culture supernatant of ATP group was also reduced after GSDME knockdown as compared with negative control siRNA (Fig. 6d). In other words, inhibition of GSDME-NT production by genetic knockdown or caspase inhibition suppressed ATP-induced pyroptosis. Together, these results demonstrated that the activation of GSDME contributed, at least partly, to ATP-induced lytic cell death in murine macrophages.

Discussion

In this study, we found that ATP induced an alternative form of pyroptosis in macrophages with blockade of the NLRP3 pathway, which was distinct from the canonical pyroptosis following NLRP3 inflammasome activation in view of their different occurrence time and mechanisms (Fig. 7). The canonical pyroptosis usually occurs within 1–2 h upon inflammasome activation, but the alternative pyroptosis in this study was delayed. Despite of this, the cells undergoing alternative pyroptosis by ATP resembled the morphological features of canonical pyroptosis with cellular ballooning both in RAW 264.7 cells and in BMDMs treated with MCC950 (an NLRP3-specific inhibitor). Apoptotic caspases (especially caspase-3) were activated during this process leading to the generation of GSDME-NT (37 kDa) but not GSDMD-NT (32 kDa). Besides ATP, nigericin could also induce similar lytic cell death in BMDMs and in THP-1-derived macrophages. In line with this, GSDME knockdown or caspase-3 inhibition significantly decreased the cell death in macrophages. All these data indicated that the canonical NLRP3 activators (e.g., ATP and nigericin) were able to induce alternative pyroptosis in macrophages dependently on the activation of apoptotic caspases and GSDME cleavage, instead of caspase-1 and GSDMD activation, when the canonical NLRP3 inflammasome pathway was blocked.

One major finding of this study is that ATP triggered a transition of GSDMD-dependent pyroptosis into GSDMD-independent pyroptosis in macrophages with the NLRP3 pathway being blocked. Basically, this is consistent with several recent observations showing that alternative forms of cell death other than GSDMD-dependent pyroptosis take place in macrophages or bone marrow-derived dendritic cells that have deficiency in canonical inflammasome pathways [14, 39–41]. In wild type macrophages, caspase-1 protease activity prevents the activation of caspase-8 and induction of apoptosis [40], whereas in caspase-1-deficient macrophages, triggering of NLRP1b and NLRC4 sensors induces ASC/caspase-8-depdendent apoptosis as an alternative form of cell death [40, 41]. In vitro, NLRC4/caspase-8-mediated apoptotic cells may eventually undergo secondary necrosis (or pyroptosis) as evidenced by loss of plasma membrane integrity [41]. Moreover, in RAW 264.7 cells reconstructed with ASC expression, GSDMD-deficiency leads to the activation of caspase-3, -7 and -8 upon ATP stimulation [14]. Another study showed that, in the context of NLRP3 activation, GSDMD-dependent pyroptosis prevents the activation of caspase-8, whereas in GSDMD-deficient macrophages, NLRP3 activation triggers delayed lytic cell death named secondary pyroptosis which is dependent on apoptotic caspases including caspase-8 and -3 [39]. Reciprocally to GSDMD-mediated suppression of caspase-8 activation, caspase-3 activation cleaves GSDMD at residue D88 (D87 in humans) to generate fragments without the pore-forming activity, highlighting a critical interconnection between pyroptosis and apoptosis. Our data are in line with these observations, adding another form of cell death transition under circumstances of the suppression of conventional NLRP3 inflammasome activation. We found that in ASC-deficient RAW 264.7 cells and BMDMs treated with MCC950, ATP induced an alternative form of pyroptosis which was accompanied by the activation of multiple apoptotic caspases including caspase-3, -7, -8, and -9. This lytic form of cell death seemed independent of GSDMD cleavage but was associated with caspase-3-mediated GSDME cleavage, leading to the production of pore-forming GSDME-NT to execute pyroptosis. Besides, necroptosis (another lytic cell death mechanistically different from pyroptosis) might not have occurred in the context of this

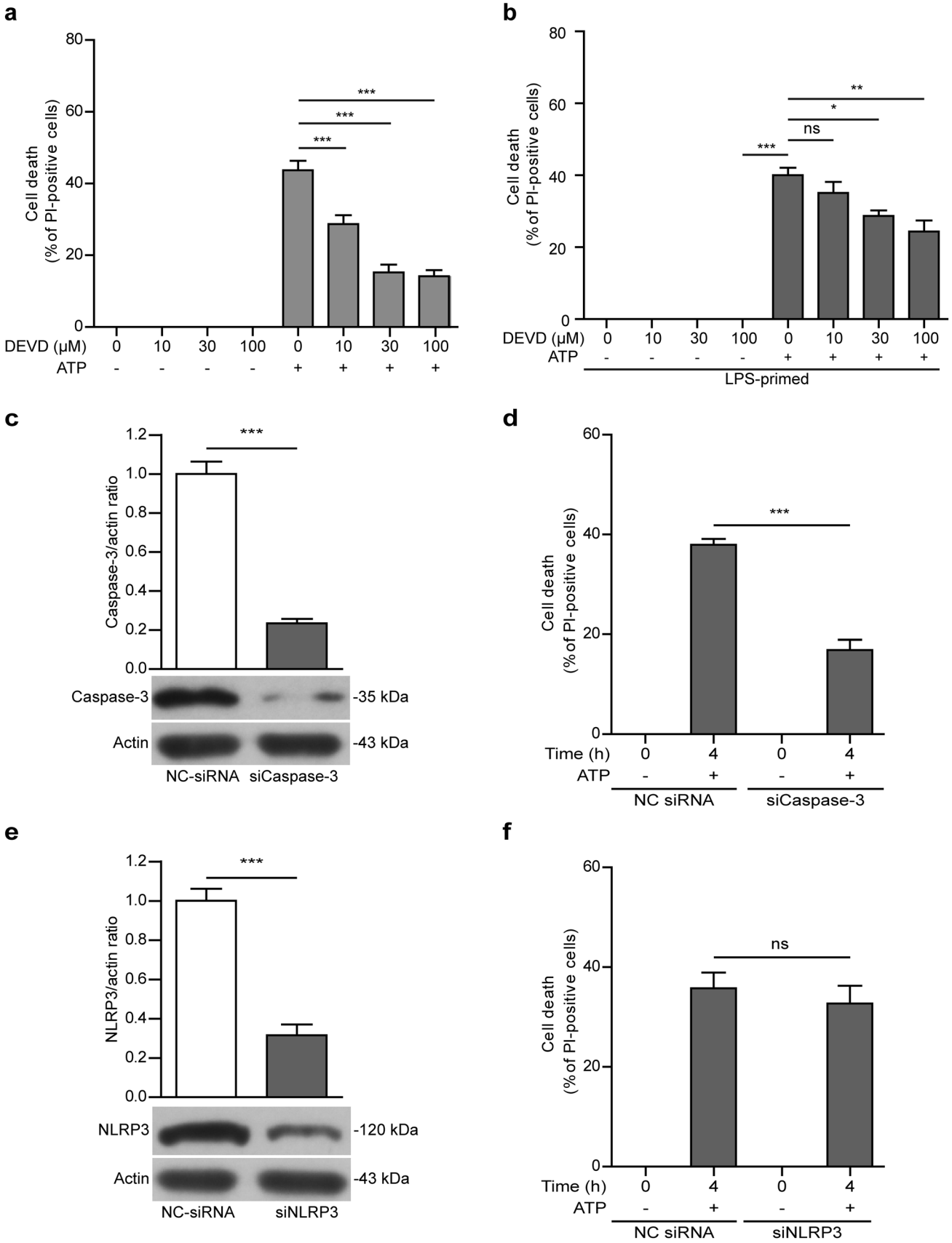
a
Cell death (% of PI-positive cells)
80
60
40
20
0
***
***
***
DEVD (μM) 0 10 30 100 0 10 30 100
ATP - - - - + + + +
b
Cell death (% of PI-positive cells)
80
60
40
20
0
**
*
ns
***
DEVD (μM) 0 10 30 100 0 10 30 100
ATP - - - - + + + +
LPS-primed
c
Caspase-3/actin ratio
1.2
1.0
0.8
0.6
0.4
0.2
0.0
***
Caspase-3
-35 kDa
Actin
-43 kDa
NC-siRNA siCaspase-3
d
Cell death (% of PI-positive cells)
60
40
20
0
***
Time (h) 0 4 0 4
ATP - + - +
NC siRNA
siCaspase-3
e
NLRP3/actin ratio
1.2
1.0
0.8
0.6
0.4
0.2
0.0
***
NLRP3
-120 kDa
Actin
-43 kDa
NC-siRNA siNLRP3
f
Cell death (% of PI-positive cells)
60
40
20
0
ns
Time (h) 0 4 0 4
ATP - + - +
NC siRNA
siNLRP3

◂**Fig. 5** Involvement of caspase-3 but not NLRP3 in ATP-induced lytic cell death in RAW 264.7 cells. **a, b** Cells were pre-treated with indicated concentrations of caspase-3 inhibitor Ac-DEVD-CHO (DEVD) for 1 h, followed by stimulation with ATP (2 mM) for 4 h. Cell death was assayed by propidum iodide (PI) staining, and observed by fluorescent microscopy. PI-positive cells in five randomly chosen fields (from 5 wells) each containing ~ 100 cells were quantified and shown as histograms. The percentage of lytic cell death is defined as the ratio of PI-positive cells relative to all cells. Data are presented as mean ± SD ($n = 5$). Statistical significance was analyzed by one-way ANOVA followed by Tukey post hoc test. $^{*}P < 0.05$; $^{***}P < 0.001$; ns, not significant. **c, d** RAW 264.7 cells were transfected with NC-siRNA or caspase-3 siRNA, respectively and then treated with ATP (2 mM) for 4 h. Cell death was assayed by PI staining. **e, f** For NLRP3 knockdown, RAW 264.7 cells were primed with LPS and then transfected with siRNA. The cells were stimulated with ATP (2 mM) for 4 h. Cell death was assayed by PI staining. PI-positive cells in five randomly chosen fields each containing ~ 100 cells were quantified and shown as histograms. The percentage of lytic cell death is defined as the ratio of PI-positive cells relative to all cells. Data are presented as mean ± SD ($n = 5$). Statistical significance was analyzed by Student's t-test (two tailed). $^{***}P < 0.001$, *ns* Not significant

study considering that caspase-8 was robustly activated and that caspase-8 prevents RIPK3–MLKL-dependent necroptosis [42].

GSDME/DFNA5 has recently been identified as a critical executor of chemotherapy drug-induced pyroptosis/secondary necrosis owing to the pore-forming activity of GSDME-NT similar to GSDMD-NT in the plasma membrane [24, 25]. The cleavage of GSDME is mediated by activated caspase-3, which produces the GSDME-NT fragment thus switching the cell death mode from apoptosis to pyroptotic cell death in chemotherapy drug-treated cells with sufficient GSDME expression [24]. Our data are in line with these studies. We showed that GSDME was constitutively expressed in macrophages. Corresponding to the activation of caspase-3, GSDME was cleaved to generate GSDME-NT fragment (37 kDa) upon ATP stimulation. Accompanied by the activation of caspase-3 and GSDME, lytic cell death resembling the phenotype of canonical pyroptosis was observed. However, this phenomenon took place only when the canonical NLRP3 pathway was blocked, either due to ASC deficiency (in RAW 2647 cells) or by NLRP3 inhibition (with MCC950 in BMDMs). Thus, our results suggested that caspase-3-mediated cleavage of GSDME contributed to ATP-induced pyroptotic cell death in macrophages with the NLRP3 pathway being blocked. However, other caspase-3 substrates than GSDME may also be involved in this process since the inhibition of ATP-induced lytic cell death by caspase-3 knockdown appeared more pronounced than that by GSDME knockdown (Figs. 5, 6). In support of this notion, recent study reported that GSDME is dispensable for the secondary necrosis that follows NLRC4-mediated apoptosis in macrophages [41]. Further investigation is therefore warranted to clarify this issue.

It is intriguing to learn what the cause was leading to the activation of caspase-8 and -9. In our study, both intrinsic (caspase-9) and extrinsic (caspase-8) apoptosis pathways were activated by ATP in RAW 264.7 cells and MCC950-treated BMDMs. It is well known that ATP can induce K^+ efflux in macrophages [7, 9, 43]. ATP binds to P2X7R and triggers cation (e.g., Na^+ and Ca^{2+}) influx resulting in TWIK2-mediated K^+ efflux [9]. It has been known that mitochondria can sense the perturbation of intracellular K^+, leading to mitochondrial dysfunction and apoptosis [44]. Upon triggering by ATP, oxidized mitochondrial DNA is released from mitochondria into the cytosol to bind and activate NLRP3 inflammasome [45, 46]. Thus, ATP-induced NLRP3 inflammasome activation seems to be downstream of mitochondrial dysfunction in macrophages. Under the setting of NLRP3 pathway blockade, the rapidly occurred NLRP3-mediated pyroptosis is blocked, whereas mitochondrial dysfunction may still be able to activate the mitochondrion-mediated intrinsic apoptosis pathway (indicated by active caspase-9), since ATP induces loss of inner mitochondrial membrane potential (loss of which is a surrogate marker of apoptosis [47]) being independent of both NLRP3 and caspase-1 [46].

However, it is largely unknown how the extrinsic apoptosis pathway (caspase-8) is activated by ATP considering previous findings that caspase-8 activation requires ASC-based inflammasome platform [39, 48–50]. Caspase-8 can be activated via the extrinsic apoptotic pathway in which ligand binding with death receptors can trigger the formation of the death receptor complex that activates caspase-8 [42]. However, it has been shown that FAS-mediated activation of caspase-8 in macrophages and dendritic cells, leading to the maturation of IL-1β and IL-18, is independent of the inflammasome components NLRP3 and ASC [51]. In BMDMs, we found that ATP induced ASC specks which were co-localized with caspase-8. Blockade of NLRP3 activation by MCC950 abrogated ASC speck formation, but caspase-8 could still be activated. In ASC-deficient RAW 264.7 cells, caspase-8 was also activated by ATP. These results suggested that ASC specks were dispensable for caspase-8 activation in our experimental setting. Although previous studies showed that activated caspase-8 can induce release of IL-1β [39, 51, 52], we found that ATP induced minimal release of IL-1β in MCC950-treated BMBMs. One possible explanation is that MCC950 had prevented the formation of NLRP3/ASC platform, which may be required for caspase-8 to mediate IL-1β maturation and release. In support of this notion, MCC950 had been shown to inhibit IL-1β release concomitant with the loss of ASC speck formation during BH3-mimetic ABT-737 plus cycloheximide-mediated apoptosis [52]. Besides, although both caspase-8 and caspase-9 were activated in our study, further research is needed to

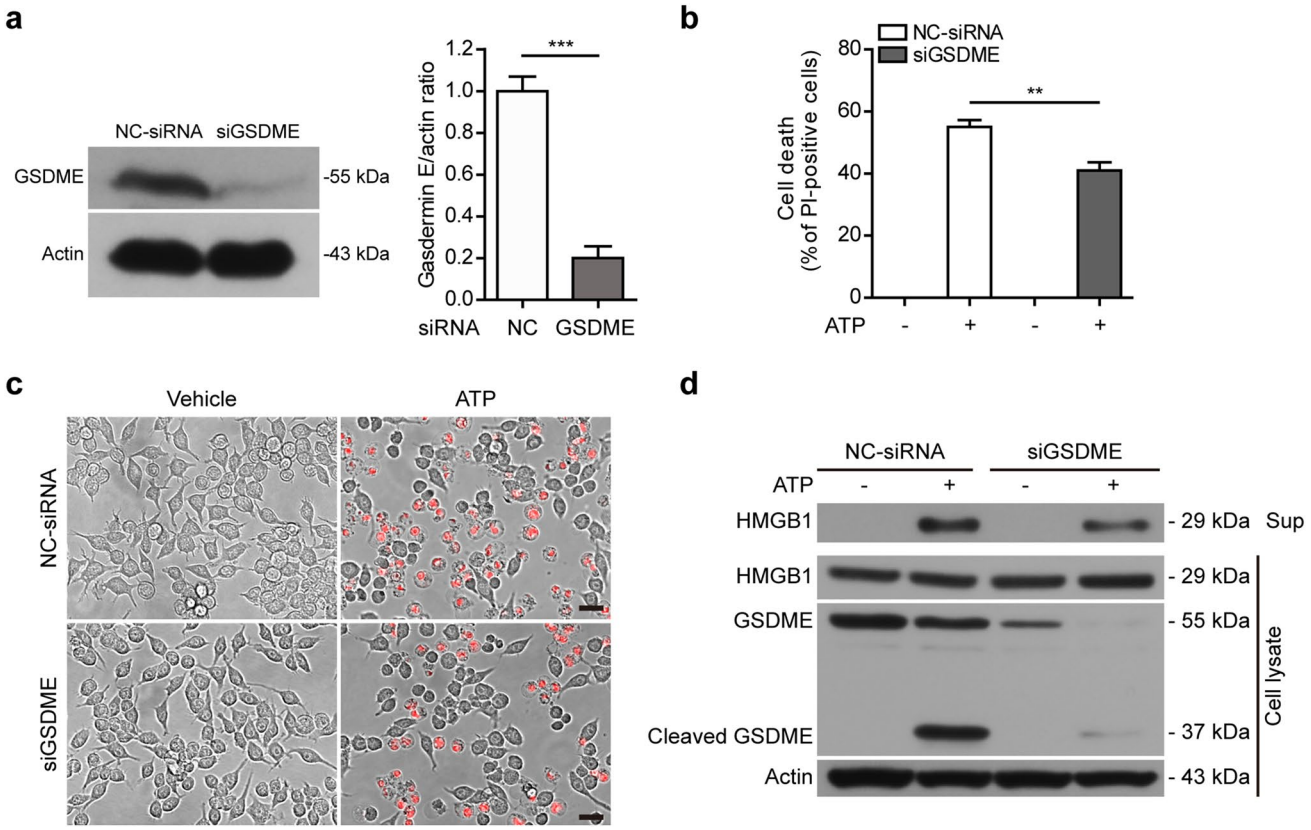

Fig. 6 *Gasdermin E* (*GSDME*) knockdown inhibited ATP-induced lytic cell death. RAW 264.7 cells were transfected with negative control (NC) siRNA or *GSDME*-specific siRNA for 48 h. The cells were then stimulated with extracellular ATP (2 mM) for 4 h. **a** Cell lysates was analyzed for the efficiency of *GSDME* knockdown by western blotting (left). Actin was used as a loading control. Histograms (right) show the quantification of GSDME levels relative to actin ($n=3$). **b, c** Cell death was assayed by PI staining, and PI fluorescence (red) was captured by fluorescence microscopy and merged with bright-field images. PI-positive cells in five randomly chosen fields each containing ~ 100 cells were quantified (**b**). The percentage of lytic cell death is defined as the ratio of PI-positive cells relative to all cells. Data are shown as mean ± SD ($n=5$). Statistical significance was analyzed by one-way ANOVA followed by Tukey post hoc test. $^{**}P<0.01$; $^{***}P<0.001$. One representative set of images of three independently performed experiments is shown (**c**). Scale bars, 20 μm. **d** Western blotting was used to evaluate the expression and secretion levels of GSDME, cleaved GSDME, and HMGB1 in cell lysates. The levels of HMGB1 in the culture supernatants were also assayed. Actin was used as a loading control for cell lysates. *NC* Negative control, *Sup* Supernatant (Color figure online)

explore which caspase plays a major role in inducing caspase-3 activation and GSDME-mediated cell death.

On the other hand, although caspase-8 prevents RIPK3–MLKL-dependent necroptosis [42], emerging evidence suggests that caspase-8 has important roles in inflammatory responses in macrophages infected with diverse pathogens. When the caspase-1 pathway is blocked or deleted, caspase-8 activation may serve as a backup mechanism [37, 53]. Recent studies showed that inhibition of TAK1 activity by *Yersinia* effector protein YopJ triggers the activation of caspase-8 leading to GSDMD and GSDME cleavage to elicit pyroptosis during *Yersinia* infection [54, 55]. The cleavage of GSDME is dependent on caspase-3 activation downstream of caspase-8 [55]. Therefore, under the conditions that canonical inflammasome activation is suppressed by pathogens [26, 27], such caspase-3-mediated pyroptotic cell death may still take place as a backup mechanism to promote innate immune responses against infections. Consistent with this hypothesis, our data indicated that caspase-8 and -3 were activated to elicit GSDME-mediated pyroptosis when the NLRP3/ASC pathway was blocked (thus with caspase-1 activation being blocked). Although our experiments were performed in RAW 264.7 cells in which NLRP3 inflammasome pathway is blocked due to deficiency of a key component ASC, and in BMDMs treated with MCC950 to suppress NLRP3 activation, the data is still of interest. ATP induced the activation of apoptotic caspases including caspase-8/-9/-3 leading to an alternative pyroptosis and release

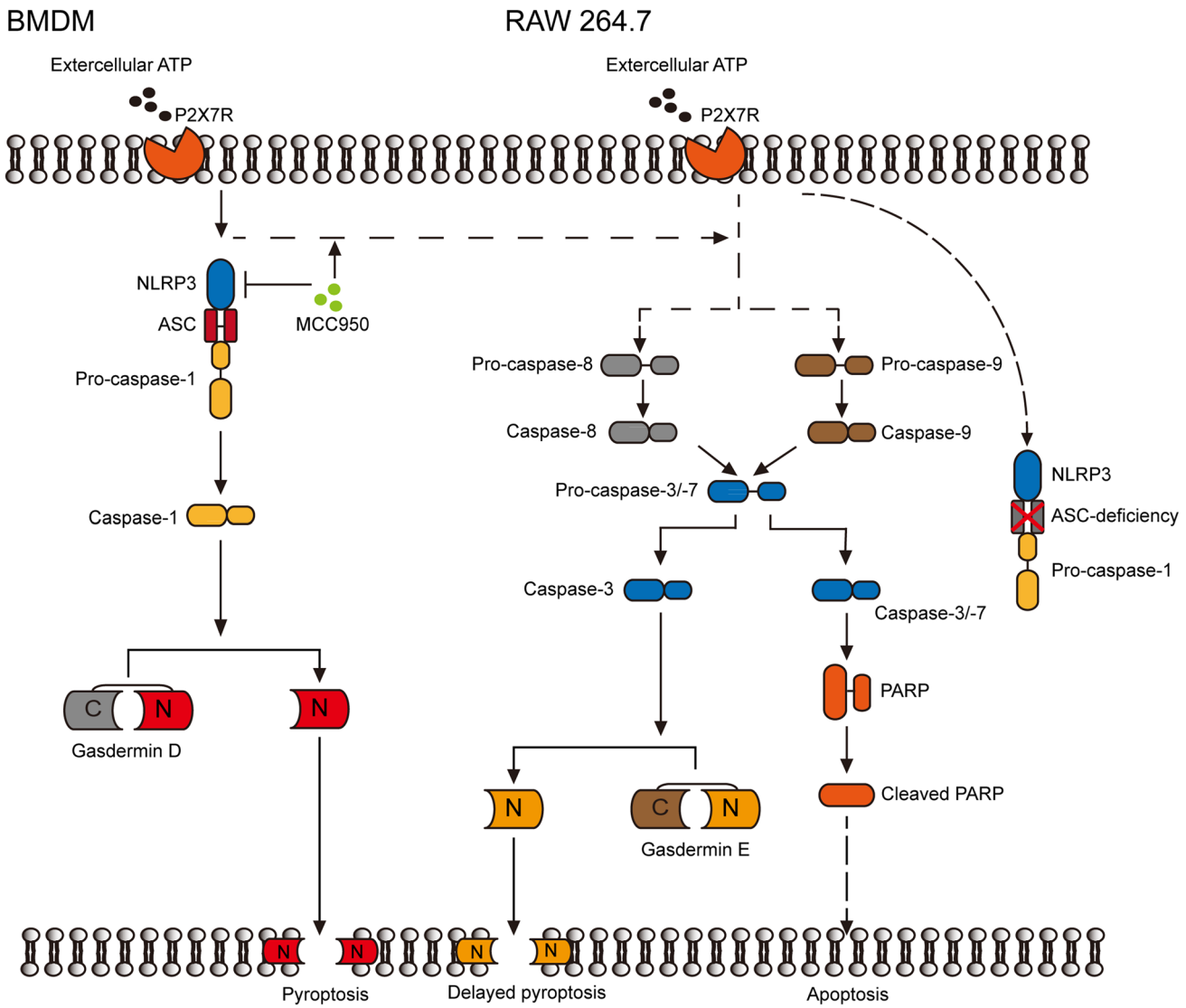

Fig. 7 Schematic depicting the action mechanisms for induction of pyroptosis by ATP in bone marrow-derived macrophages (BMDMs) and RAW 264.7 cell line. In RAW 264.7 cells deficient in ASC, ATP induced a delayed form of pyroptotic cell death partly reliant on GSDME cleavage (right panel). In BMDMs, ATP induces rapid pyroptosis mediated by gasdermin D cleavage, whereas it induced delayed pyroptosis associated with gasdermin E cleavage when the canonical NLRP3 pathway has been blocked (left panel)

of proinflammatory factors such as HMGB1, corroborating the possibility to induce robust inflammation. It is therefore likely that such pyroptosis may intensify innate immunity of the host to combat against pathogen evasion. Yet, more investigation especially an appropriate animal model is warranted to verify this hypothesis.

In summary, our study showed that ATP was able to induce an alternative pyroptosis in macrophages in which the NLRP3-mediated rapid pyroptosis had been blocked, highlighting another form of interplay between pyroptosis and apoptosis pathways. Considering that ATP is an important DAMP during tissue injury or infections [56], further research is warranted to explore the in vivo relevance in an appropriate animal model of pathogenic infection where inflammasome activation has been blocked or suppressed.

Acknowledgements This work was supported by the grants from the National Natural Science Foundation of China (Grant Nos. 81773965, 81673664 and 81873064).

Compliance with ethical standards

Conflicts of interest The authors declare no conflicts of interest.

References

1. Medzhitov R (2008) Origin and physiological roles of inflammation. Nature 454:428–435. https://doi.org/10.1038/nature07201
2. Takeuchi O, Akira S (2010) Pattern recognition receptors and inflammation. Cell 140:805–820. https://doi.org/10.1016/j.cell.2010.01.022
3. Lamkanfi M, Dixit VM (2014) Mechanisms and functions of inflammasomes. Cell 157:1013–1022. https://doi.org/10.1016/j.cell.2014.04.007
4. Kono H, Onda A, Yanagida T (2014) Molecular determinants of sterile inflammation. Curr Opin Immunol 26:147–156. https://doi.org/10.1016/j.coi.2013.12.004
5. Davies LC, Jenkins SJ, Allen JE, Taylor PR (2013) Tissue-resident macrophages. Nat Immunol 14:986–995. https://doi.org/10.1038/ni.2705
6. de Zoete MR, Palm NW, Zhu S, Flavell RA (2014) Inflammasomes. Cold Spring Harb Perspect Biol 6:a016287. https://doi.org/10.1101/cshperspect.a016287
7. He Y, Hara H, Nunez G (2016) Mechanism and regulation of NLRP3 inflammasome activation. Trends Biochem Sci 41:1012–1021. https://doi.org/10.1016/j.tibs.2016.09.002
8. Mariathasan S, Weiss DS, Newton K, McBride J, O'Rourke K, Roose-Girma M, Lee WP, Weinrauch Y, Monack DM, Dixit VM (2006) Cryopyrin activates the inflammasome in response to toxins and ATP. Nature 440:228–232. https://doi.org/10.1038/nature04515
9. Di A, Xiong S, Ye Z, Malireddi RKS, Kometani S, Zhong M, Mittal M, Hong Z, Kanneganti TD, Rehman J, Malik AB (2018) The TWIK2 potassium efflux channel in macrophages mediates NLRP3 inflammasome-induced inflammation. Immunity 49(56–65):e54. https://doi.org/10.1016/j.immuni.2018.04.032
10. Shi J, Zhao Y, Wang K, Shi X, Wang Y, Huang H, Zhuang Y, Cai T, Wang F, Shao F (2015) Cleavage of GSDMD by inflammatory caspases determines pyroptotic cell death. Nature 526:660–665. https://doi.org/10.1038/nature15514
11. Kayagaki N, Stowe IB, Lee BL et al (2015) Caspase-11 cleaves gasdermin D for non-canonical inflammasome signalling. Nature 526:666–671. https://doi.org/10.1038/nature15541
12. Liu X, Zhang Z, Ruan J, Pan Y, Magupalli VG, Wu H, Lieberman J (2016) Inflammasome-activated gasdermin D causes pyroptosis by forming membrane pores. Nature 535:153–158. https://doi.org/10.1038/nature18629
13. Ding J, Wang K, Liu W, She Y, Sun Q, Shi J, Sun H, Wang DC, Shao F (2016) Pore-forming activity and structural autoinhibition of the gasdermin family. Nature 535:111–116. https://doi.org/10.1038/nature18590
14. He WT, Wan H, Hu L, Chen P, Wang X, Huang Z, Yang ZH, Zhong CQ, Han J (2015) Gasdermin D is an executor of pyroptosis and required for interleukin-1beta secretion. Cell Res 25:1285–1298. https://doi.org/10.1038/cr.2015.139
15. Chen X, He WT, Hu L, Li J, Fang Y, Wang X, Xu X, Wang Z, Huang K, Han J (2016) Pyroptosis is driven by non-selective gasdermin-D pore and its morphology is different from MLKL channel-mediated necroptosis. Cell Res 26:1007–1020. https://doi.org/10.1038/cr.2016.100
16. Sborgi L, Ruhl S, Mulvihill E, Pipercevic J, Heilig R, Stahlberg H, Farady CJ, Muller DJ, Broz P, Hiller S (2016) GSDMD membrane pore formation constitutes the mechanism of pyroptotic cell death. EMBO J 35:1766–1778. https://doi.org/10.15252/embj.201694696
17. Aglietti RA, Estevez A, Gupta A, Ramirez MG, Liu PS, Kayagaki N, Ciferri C, Dixit VM, Dueber EC (2016) GsdmD p30 elicited by caspase-11 during pyroptosis forms pores in membranes. Proc Natl Acad Sci USA 113:7858–7863. https://doi.org/10.1073/pnas.1607769113
18. Evavold CL, Ruan J, Tan Y, Xia S, Wu H, Kagan JC (2018) The pore-forming protein gasdermin D regulates interleukin-1 secretion from living macrophages. Immunity 48(35–44):e36. https://doi.org/10.1016/j.immuni.2017.11.013
19. Zhang Y, Chen X, Gueydan C, Han J (2018) Plasma membrane changes during programmed cell deaths. Cell Res 28:9–21. https://doi.org/10.1038/cr.2017.133
20. Wallach D, Kang TB, Dillon CP, Green DR (2016) Programmed necrosis in inflammation: Toward identification of the effector molecules. Science 352:aaf2154. https://doi.org/10.1126/science.aaf2154
21. Jorgensen I, Miao EA (2015) Pyroptotic cell death defends against intracellular pathogens. Immunol Rev 265:130–142. https://doi.org/10.1111/imr.12287
22. Shi J, Gao W, Shao F (2017) Pyroptosis: gasdermin-mediated programmed necrotic cell death. Trends Biochem Sci 42:245–254. https://doi.org/10.1016/j.tibs.2016.10.004
23. Galluzzi L, Vitale I, Aaronson SA et al (2018) Molecular mechanisms of cell death: recommendations of the nomenclature committee on cell death 2018. Cell Death Differ 25:486–541. https://doi.org/10.1038/s41418-017-0012-4
24. Wang Y, Gao W, Shi X, Ding J, Liu W, He H, Wang K, Shao F (2017) Chemotherapy drugs induce pyroptosis through caspase-3 cleavage of a gasdermin. Nature 547:99–103. https://doi.org/10.1038/nature22393
25. Rogers C, Fernandes-Alnemri T, Mayes L, Alnemri D, Cingolani G, Alnemri ES (2017) Cleavage of DFNA5 by caspase-3 during apoptosis mediates progression to secondary necrotic/pyroptotic cell death. Nat Commun 8:14128. https://doi.org/10.1038/ncomms14128
26. Stewart MK, Cookson BT (2016) Evasion and interference: intracellular pathogens modulate caspase-dependent inflammatory responses. Nat Rev Microbiol 14:346–359. https://doi.org/10.1038/nrmicro.2016.50
27. Ulland TK, Ferguson PJ, Sutterwala FS (2015) Evasion of inflammasome activation by microbial pathogens. J Clin Investig 125:469–477. https://doi.org/10.1172/jci75254
28. LaRock CN, Cookson BT (2012) The Yersinia virulence effector YopM binds caspase-1 to arrest inflammasome assembly and processing. Cell Host Microbe 12:799–805. https://doi.org/10.1016/j.chom.2012.10.020
29. Dorfleutner A, Talbott SJ, Bryan NB, Funya KN, Rellick SL, Reed JC, Shi X, Rojanasakul Y, Flynn DC, Stehlik C (2007) A shope fibroma virus PYRIN-only protein modulates the host immune response. Virus Genes 35:685–694. https://doi.org/10.1007/s11262-007-0141-9
30. Johnston JB, Barrett JW, Nazarian SH, Goodwin M, Ricciuto D, Wang G, McFadden G (2005) A poxvirus-encoded pyrin domain protein interacts with ASC-1 to inhibit host inflammatory and apoptotic responses to infection. Immunity 23:587–598. https://doi.org/10.1016/j.immuni.2005.10.003
31. Coll RC, Robertson AA, Chae JJ et al (2015) A small-molecule inhibitor of the NLRP3 inflammasome for the treatment of inflammatory diseases. Nat Med 21:248–255. https://doi.org/10.1038/nm.3806
32. Li CG, Yan L, Jing YY, Xu LH, Liang YD, Wei HX, Hu B, Pan H, Zha QB, Ouyang DY, He XH (2017) Berberine augments ATP-induced inflammasome activation in macrophages by enhancing AMPK signaling. Oncotarget 8:95–109. https://doi.org/10.18632/oncotarget.13921
33. Py BF, Jin M, Desai BN, Penumaka A, Zhu H, Kober M, Dietrich A, Lipinski MM, Henry T, Clapham DE, Yuan J (2014)

Caspase-11 controls interleukin-1beta release through degradation of TRPC1. Cell Rep 6:1122–1128. https://doi.org/10.1016/j.celrep.2014.02.015
34. Li CG, Yan L, Mai FY, Shi ZJ, Xu LH, Jing YY, Zha QB, Ouyang DY, He XH (2017) Baicalin inhibits NOD-like receptor family, pyrin containing domain 3 inflammasome activation in murine macrophages by augmenting protein kinase a signaling. Front Immunol 8:1409. https://doi.org/10.3389/fimmu.2017.01409
35. Kayagaki N, Warming S, Lamkanfi M, Vande Walle L, Louie S, Dong J, Newton K, Qu Y, Liu J, Heldens S, Zhang J, Lee WP, Roose-Girma M, Dixit VM (2011) Non-canonical inflammasome activation targets caspase-11. Nature 479:117–121. https://doi.org/10.1038/nature10558
36. Liu Y, Jing YY, Zeng CY, Li CG, Xu LH, Yan L, Bai WJ, Zha QB, Ouyang DY, He XH (2017) Scutellarin suppresses NLRP3 inflammasome activation in macrophages and protects mice against bacterial sepsis. Front Pharmacol 8:975. https://doi.org/10.3389/fphar.2017.00975
37. Mascarenhas DPA, Cerqueira DM, Pereira MSF, Castanheira FVS, Fernandes TD, Manin GZ, Cunha LD, Zamboni DS (2017) Inhibition of caspase-1 or gasdermin-D enable caspase-8 activation in the Naip5/NLRC4/ASC inflammasome. PLoS Pathog 13:e1006502. https://doi.org/10.1371/journal.ppat.1006502
38. Pelegrin P, Barroso-Gutierrez C, Surprenant A (2008) P2X7 receptor differentially couples to distinct release pathways for IL-1beta in mouse macrophage. J Immunol 180:7147–7157. https://doi.org/10.4049/jimmunol.180.11.7147
39. Schneider KS, Gross CJ, Dreier RF et al (2017) The inflammasome drives GSDMD-independent secondary pyroptosis and IL-1 release in the absence of caspase-1 protease activity. Cell Rep 21:3846–3859. https://doi.org/10.1016/j.celrep.2017.12.018
40. Van Opdenbosch N, Van Gorp H, Verdonckt M et al (2017) Caspase-1 engagement and TLR-induced c-FLIP expression suppress ASC/caspase-8-dependent apoptosis by inflammasome sensors NLRP1b and NLRC4. Cell Rep 21:3427–3444. https://doi.org/10.1016/j.celrep.2017.11.088
41. Lee BL, Mirrashidi KM, Stowe IB, Kummerfeld SK, Watanabe C, Haley B, Cuellar TL, Reichelt M, Kayagaki N (2018) ASC- and caspase-8-dependent apoptotic pathway diverges from the NLRC4 inflammasome in macrophages. Sci Rep 8:3788. https://doi.org/10.1038/s41598-018-21998-3
42. Feltham R, Vince JE, Lawlor KE (2017) Caspase-8: not so silently deadly. Clin Transl Immunology 6:e124. https://doi.org/10.1038/cti.2016.83
43. Munoz-Planillo R, Kuffa P, Martinez-Colon G, Smith BL, Rajendiran TM, Nunez G (2013) K^+ efflux is the common trigger of NLRP3 inflammasome activation by bacterial toxins and particulate matter. Immunity 38:1142–1153. https://doi.org/10.1016/j.immuni.2013.05.016
44. Tschopp J (2011) Mitochondria: sovereign of inflammation? Eur J Immunol 41:1196–1202. https://doi.org/10.1002/eji.201141436
45. Zhong Z, Liang S, Sanchez-Lopez E, He F, Shalapour S, Lin XJ, Wong J, Ding S, Seki E, Schnabl B, Hevener AL, Greenberg HB, Kisseleva T, Karin M (2018) New mitochondrial DNA synthesis enables NLRP3 inflammasome activation. Nature. https://doi.org/10.1038/s41586-018-0372-z
46. Shimada K, Crother TR, Karlin J et al (2012) Oxidized mitochondrial DNA activates the NLRP3 inflammasome during apoptosis. Immunity 36:401–414. https://doi.org/10.1016/j.immuni.2012.01.009
47. Ly JD, Grubb DR, Lawen A (2003) The mitochondrial membrane potential (deltapsi(m)) in apoptosis; an update. Apoptosis 8:115–128. https://doi.org/10.1023/a:1022945107762
48. Antonopoulos C, El Sanadi C, Kaiser WJ, Mocarski ES, Dubyak GR (2013) Proapoptotic chemotherapeutic drugs induce noncanonical processing and release of IL-1beta via caspase-8 in dendritic cells. J Immunol 191:4789–4803. https://doi.org/10.4049/jimmunol.1300645
49. Pierini R, Juruj C, Perret M, Jones CL, Mangeot P, Weiss DS, Henry T (2012) AIM2/ASC triggers caspase-8-dependent apoptosis in francisella-infected caspase-1-deficient macrophages. Cell Death Differ 19:1709–1721. https://doi.org/10.1038/cdd.2012.51
50. Sagulenko V, Thygesen SJ, Sester DP, Idris A, Cridland JA, Vajjhala PR, Roberts TL, Schroder K, Vince JE, Hill JM, Silke J, Stacey KJ (2013) AIM2 and NLRP3 inflammasomes activate both apoptotic and pyroptotic death pathways via ASC. Cell Death Differ 20:1149–1160. https://doi.org/10.1038/cdd.2013.37
51. Bossaller L, Chiang PI, Schmidt-Lauber C, Ganesan S, Kaiser WJ, Rathinam VA, Mocarski ES, Subramanian D, Green DR, Silverman N, Fitzgerald KA, Marshak-Rothstein A, Latz E (2012) Cutting edge: FAS (CD95) mediates noncanonical IL-1beta and IL-18 maturation via caspase-8 in an RIP3-independent manner. J Immunol 189:5508–5512. https://doi.org/10.4049/jimmunol.1202121
52. Vince JE, De Nardo D, Gao W et al (2018) The mitochondrial apoptotic effectors BAX/BAK activate caspase-3 and -7 to trigger NLRP3 inflammasome and caspase-8 driven IL-1beta activation. Cell Rep 25(2339–2353):e2334. https://doi.org/10.1016/j.celrep.2018.10.103
53. Rauch I, Deets KA, Ji DX, von Moltke J, Tenthorey JL, Lee AY, Philip NH, Ayres JS, Brodsky IE, Gronert K, Vance RE (2017) NAIP-NLRC4 inflammasomes coordinate intestinal epithelial cell expulsion with eicosanoid and IL-18 release via activation of caspase-1 and -8. Immunity 46:649–659. https://doi.org/10.1016/j.immuni.2017.03.016
54. Orning P, Weng D, Starheim K et al (2018) Pathogen blockade of TAK1 triggers caspase-8-dependent cleavage of gasdermin D and cell death. Science 362:1064–1069. https://doi.org/10.1126/science.aau2818
55. Sarhan J, Liu BC, Muendlein HI, Li P, Nilson R, Tang AY, Rongvaux A, Bunnell SC, Shao F, Green DR, Poltorak A (2018) Caspase-8 induces cleavage of gasdermin D to elicit pyroptosis during Yersinia infection. Proc Natl Acad Sci USA. https://doi.org/10.1073/pnas.1809548115
56. Di Virgilio F, Dal Ben D, Sarti AC, Giuliani AL, Falzoni S (2017) The P2X7 receptor in infection and inflammation. Immunity 47:15–31. https://doi.org/10.1016/j.immuni.2017.06.020